

# Linker and Tail Group Modifications on 2-((4-isopropyl-4H-1,2,4-triazol-3-yl)thio)-N-(4-phenoxyphenyl)Acetamide to Improve SIRT2 Inhibitory Potency

Mahmut GOZELLE\*, Yesim OZKAN\*\*, Gokcen EREN\*\*\*\*

*Linker and Tail Group Modifications on 2-((4-isopropyl-4H-1,2,4-triazol-3-yl)thio)-N-(4-phenoxyphenyl)Acetamide to Improve SIRT2 Inhibitory Potency*

## SUMMARY

Interest in SIRT2 has grown continuously over recent years, resulting in accumulated evidence that overexpression of SIRT2 is associated with many disorders, and its inhibition delays the progression of pathologies. Hence, targeting SIRT2 may be of therapeutic relevance, and inhibiting SIRT2 activity is a promising therapeutic strategy for severe diseases. The overarching aim of the work presented herein was to improve the SIRT2 inhibition potentials of our initial hits by modifying both linker and tail groups. Among the title compounds, ST49 (50.07%) and ST60 (54.03%) displayed the best inhibition rates against SIRT2 over SIRT1 and SIRT3. Predicted binding conformations of these compounds to SIRT2 highlighted the impact of the crucial interactions with SIRT2 active site residues on inhibitory activity. These results would provide structural guidance for future related design efforts.

**Key Words:** Drug design, hit optimization, inhibitor, molecular modeling, SIRT2

*SIRT2 İnhibitör Etkisini Geliştirmek Amacıyla 2-((4-izopropil-4H-1,2,4-triazol-3-il)tiyo)-N-(4-fenoksifenil)Asetamid Yapısında Köprü ve Kuyruk Grupları Üzerinde Gerçekleştirilen Modifikasyonlar*

## ÖZ

SIRT2 enziminin aşırı ekspresyonunun birçok hastalık ile ilişkili olduğuna ve SIRT2 inhibisyonunun patolojilerin ilerlemesini geciktirdiğine dair çalışmaların varlığı, SIRT2 enzimine olan ilgiyi artırmıştır. Bu nedenle, SIRT2 inhibisyonu ciddi hastalıkların tedavisi için umut verici bir terapötik hedef haline gelmiştir. Bu çalışmada, daha önce bildirilen öncü bileşiğin köprü ve kuyruk grupları üzerinde yapısal modifikasyonlar yapılarak SIRT2 inhibisyon potansiyellerinin geliştirilmesi amaçlanmıştır. Sentezlenen bileşikler arasında ST49 (%50.07) ve ST60 (%54.03), SIRT1 ve SIRT3'e kıyasla SIRT2'ye karşı en iyi inhibisyonu sergilemişlerdir. Bu bileşiklerin öngörülen bağlanma konformasyonları, inhibitör etki için SIRT2 aktif bölgesindeki önemli etkileşimlerin varlığını desteklemiştir. Bu sonuçlar, gelecekteki tasarım çalışmaları için yol gösterici veriler sağlamaktadır.

**Anahtar Kelimeler:** İlaç tasarımı, öncü bileşik optimizasyonu, inhibitör, moleküler modelleme, SIRT2

Received: 04.03.2024

Revised: 19.04.2024

Accepted: 22.04.2024

\* ORCID: 0000-0003-0234-6577, SIRTeam Group, Department of Pharmaceutical Chemistry, Faculty of Pharmacy, Gazi University, 06330 Ankara, Türkiye.

\*\* ORCID: 0000-0002-1669-4962, Department of Biochemistry, Faculty of Pharmacy, Gazi University, 06330 Ankara, Türkiye.

\*\*\* ORCID: 0000-0002-3420-607X, SIRTeam Group, Department of Pharmaceutical Chemistry, Faculty of Pharmacy, Gazi University, 06330 Ankara, Türkiye.

## INTRODUCTION

Epigenetic-modifying enzymes, classified into writers, readers, and erasers, are gaining interest as a potential target for drug discovery (Biswas & Rao, 2018; Ganesan et al., 2019; Lu et al., 2020; Zhang et al., 2023). Sirtuins (SIRT) are a host of nicotinamide adenine dinucleotide (NAD<sup>+</sup>)-dependent histone deacetylases (HDACs), acting as epigenetic erasers (Biswas & Rao, 2018; Chen et al., 2015; Frye, 2000). SIRT2, the second member of the SIRT family, has predominantly cytoplasmic localization but shuttles into the nucleus to regulate nucleolar processes during mitosis (Min et al., 2018; Silva et al., 2023). SIRT2 plays a role in a wide range of physiological processes, such as metabolism and control of gene expression, through its deacylase activity on histones and non-histone proteins, including  $\alpha$ -tubulin, p53, BubR1, BCL6, FOXO1, FOXO3a, and severe proteins involved in the regulation of metabolic enzymes (Avalos et al., 2002; Jing, Gesta, & Kahn, 2007; North et al., 2003; North et al., 2014; Penteado et al., 2023; Xu et al., 2014; Zhao et al., 2013). Accordingly, the importance of SIRT2 expression levels has been uncovered in a wide range of diseases, such as cancer, neurodegeneration, inflammation, and aging (Chen, Huang, & Hu, 2020; Hong et al., 2021; Kaya & Eren, 2023; Wang et al., 2019). Although research and development of small molecule SIRT2 inhibitors have gained significant momentum (Cai et al., 2023; Eren et al., 2019; Gozelle et al., 2022; Gozelle et al., 2023; Mellini et al., 2017; Quinti et al., 2016; Rumpf et al., 2015; Spiegelman et al., 2019; Sukuroglu et al., 2021;

Tantawy et al., 2021; Trapp et al., 2006; Yagci et al., 2021; Yang et al., 2018; Yang et al., 2019), there is still a lack of clinically approved SIRT2 inhibitors and more effort should be focused on novel SIRT2 inhibitor scaffolds with improved efficacy and drug-like physicochemical properties.

Our initial attempt to identify novel scaffolds for SIRT2 inhibition let us obtain hit compounds with confirmed activities from virtual screening (Eren et al., 2019). Herein, motivated by a desire to drive further inhibitor optimization, among the obtained hits, **STH2** was selected and refined by linker and tail group modifications to improve SIRT2 inhibitory potency (Figure 1). The oxygen atom, as a linker between the phenyl ring which was accommodated in the substrate channel of SIRT2 and the central phenyl ring, was replaced by -CH<sub>2</sub>O-, -OCH<sub>2</sub>-, -NH-, -CH<sub>2</sub>NH-, -NHCH<sub>2</sub>-, -CH<sub>2</sub>-, and -CO- groups to achieve the needed orientation of terminal phenyl ring allowing the crucial  $\pi$ - $\pi$  interactions with the residues F119, F131, and F234. In the case of the tail group, which was directed toward the selectivity pocket, modification strategies, including fused ring cyclization, chain cyclization, and bioisosteric replacement, were adopted to access favorable moieties for selectivity pocket occupation, primarily by interacting with the residues Y139 and F190. As a result, fourteen novel analogs, seven of which were *N*-(4-phenoxyphenyl)aryl-carboxamides (**ST47-ST53**) and seven were *N*-(aryl)-2-(phenylthio)acetamides (**ST54-ST60**) were designed and synthesized, followed by evaluation of their inhibitory activities against SIRT2.

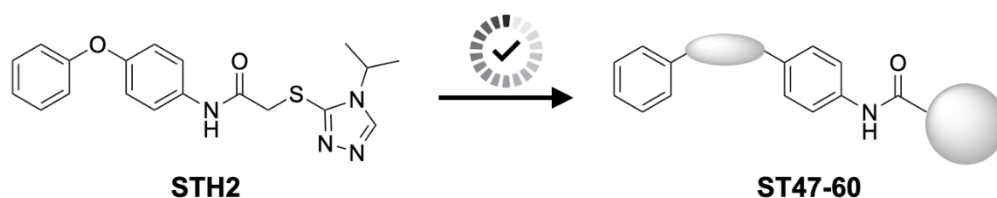


**Figure 1.** Structural modifications on **STH2** yielding novel analogues **ST47-60**.

## MATERIAL AND METHODS

### Chemistry

All chemicals used in the research were purchased commercially and employed without additional purification. Thin-layer chromatography (TLC) was applied to observe reactions on silica-coated aluminum plates (Silica gel 60 F<sub>254</sub>, Merck) using UV light at 254 or 365 nm wavelengths. Using tetramethylsilane as the internal standard, <sup>1</sup>H-NMR and <sup>13</sup>C-NMR spectra were obtained using a Bruker Avance neo 500 MHz FT-NMR and an Agilent Varian Mercury 400 MHz High-Performance Digital FT-NMR spectrometers. The chemical shifts were identified as δ (ppm), whereas the coupling constants were expressed as Hertz. The Waters LCT Premier XE Mass Spectrometer was used to acquire high-resolution mass spectra data (HRMS). The equipment was utilized in electrospray ionization (ESI<sup>+</sup>) mode and connected to an AQUITY Ultra Performance Liquid Chromatography system (Waters Corporation, Milford, MA, USA) with a UV detector set to monitor at 254 nm wavelength. The purity of all target compounds exceeded 95%. The melting points were determined using the Stuart SMP50 automated melting point instrument without correction.

4-Phenoxyaniline (1a): The synthesis of 1a was performed as previously reported (Lanning et al., 2016; Ma & Rao, 2003; Yagci et al., 2021). Yield: 37%, white solid. Mp 84.1-84.4 °C. CAS: 139-59-3. HRMS (ESI/TOF) *m/z*: [M+ACN+H]<sup>+</sup> Calcd for C<sub>14</sub>H<sub>15</sub>N<sub>2</sub>O 227.1184; Found 227.1182.

2-Bromo-*N*-(4-phenoxyphenyl)acetamide (1b): The synthesis of 1b was performed as previously reported (Han et al., 2012). Yield: 55%, white solid. Mp 109.5-109.9 °C. CAS: 36160-85-7. HRMS (ESI/TOF) *m/z*: [M+H]<sup>+</sup> Calcd for C<sub>14</sub>H<sub>13</sub>BrNO<sub>2</sub> 306.0130; Found 306.0121.

2-(Phenylthio)acetic acid (2a): The synthesis of 2a was performed as previously reported (Xie et al., 2017). Yield: 85%, white solid. Mp 60.0-60.9 °C. CAS: 103-04-8. HRMS (ESI/TOF) *m/z*: [M+ACN+H]<sup>+</sup> Calcd for C<sub>8</sub>H<sub>9</sub>O<sub>2</sub>S 210.0589; Found 210.0587.

*N*-(4-Aminophenyl)-2-(phenylthio)acetamide (2b): Initially, *N*-(4-nitrophenyl)-2-(phenylthio)acetamide (CAS: 220518-16-1) was synthesized by amidation of 2a (1 mmol) and 4-nitroaniline (1 mmol) in the presence of oxalyl chloride by using described method by Gozelle et al. (2022). Next, *N*-(4-nitrophenyl)-2-(phenylthio)acetamide (1 mmol), without performing additional purification, was refluxed in ethanol for 6 h in the presence of SnCl<sub>2</sub>·H<sub>2</sub>O (5 mmol). After the reaction was finished, the reaction mixture was concentrated *in vacuo*, and the crude was dissolved in a 10% aqueous solution NaHCO<sub>3</sub> solution. The aqueous phase was extracted with ethyl acetate (3x10 ml), and the organic phase was subjected to washing with brine. After being dried over anhydrous Na<sub>2</sub>SO<sub>4</sub>, the organic phase was concentrated *in vacuo*. The pure 2b was obtained by purifying the crude product via silica-based column chromatography using an elution system of *n*-hexane:ethyl acetate (80:20). Yield: 61%, white solid. Mp >300 °C. CAS: 1019393-66-8. HRMS (ESI/TOF) *m/z*: [M+H]<sup>+</sup> Calcd for C<sub>14</sub>H<sub>15</sub>N<sub>2</sub>OS 259.0905; Found 259.0905.

*N*-(4-formylphenyl)-2-(phenylthio)acetamide (2c): Oxalyl chloride (2 mmol) was added to a solution of 2a (1 mmol) and a catalytic amount of DMF in DCM at 0 °C, and the reaction mixture was stirred at room temperature for 2 h. The solvent was removed *in vacuo* after acyl chloride was formed. A solution of obtained 2-(phenylthio)acetyl chloride (theoretically 1 mmol) in DCM was added dropwise to a solution of 4-aminobenzaldehyde (1 mmol) and DIPEA (1.5 mmol) in DCM at 0 °C and stirred at room temperature for 4 h. Without additional purification. The resulting 2c was used in the following step. Yield: 45%, yellowish oil. CAS: 1977315-84-6. HRMS (ESI/TOF) *m/z*: [M+H]<sup>+</sup> Calcd for C<sub>15</sub>H<sub>14</sub>NO<sub>2</sub>S 272.0745; Found 272.0737.

General synthesis method A through acyl chloride-mediated amide formation (ST47, ST48, ST52-ST56, ST59, ST60): Oxalyl chloride (2 mmol) was added to a solution of an appropriate carboxylic acid (1 mmol), and a catalytic amount of DMF in DCM at 0

°C. Then, the mixture was stirred for 2 h at room temperature. The solvent was removed *in vacuo* after acyl chloride was formed. A solution of obtained appropriate acyl chloride (theoretically 1 mmol) in DCM was added dropwise to a solution of an appropriate amine (1 mmol) and DIPEA (1.5 mmol) in DCM at 0 °C. The mixture was stirred at room temperature for 2-4 h. After the reaction was completed, the reaction mixture was diluted with DCM and subjected to sequential washing with 0.1 M HCl, 1% aqueous solution of NaHCO<sub>3</sub>, and brine. After being dried over anhydrous Na<sub>2</sub>SO<sub>4</sub>, the combined organic phase was concentrated *in vacuo*. While ST47, ST48, and ST53 were purified by recrystallization from ethanol/water, ST52, ST54, ST55, ST56, ST59, and ST60 were purified by silica-based column chromatography using an elution system of *n*-hexane:ethyl acetate (85:15).

General synthesis method B through EDC/HOBt-mediated amide formation (ST50, ST51): A solution of an appropriate carboxylic acid (1 mmol), HOBt (1 mmol), EDC (1 mmol), and DIPEA (1.5 mmol) in DCM was stirred at room temperature for 30 min. After adding 1a (1 mmol), the reaction mixture was stirred overnight at room temperature until the reaction was completed. Then, the reaction mixture was diluted with DCM and subjected to sequential washing with 0.1 M HCl, 1% aqueous solution of NaHCO<sub>3</sub>, and brine. After being dried over anhydrous Na<sub>2</sub>SO<sub>4</sub>, the combined organic phase was concentrated *in vacuo*. The crude product underwent purification via silica-based column chromatography using an elution system of *n*-hexane:ethyl acetate (85:15).

*N*-(4-Phenoxyphenyl)-3-phenylpropanamide (ST47): Obtained following the general synthesis method A from 3-phenylpropanoyl chloride (theoretically 1 mmol), 1a (1 mmol), and DIPEA (1.5 mmol). Yield: 45%, white solid. Mp 133.4-133.7 °C. <sup>1</sup>H NMR (CDCl<sub>3</sub>, 400 MHz): δ 7.37 (d, *J*=9.2 Hz, 2H), 7.27-7.33 (m, 4H), 7.19-7.25 (m, 3H), 7.14 (br s, 1H), 7.07 (t, *J*=7.4 Hz, 1H), 6.92-6.97 (m, 4H), 3.04 (t, *J*=7.6 Hz, 2H), 2.65 (t, *J*=7.6 Hz, 2H). <sup>13</sup>C-NMR (CDCl<sub>3</sub>, 100 MHz): δ 170.3, 157.5, 153.5, 140.6, 133.2, 129.7, 128.4,

128.4, 126.4, 123.1, 121.8, 119.5, 118.4, 39.3, 31.6. HRMS (ESI/TOF) *m/z*: [M+H]<sup>+</sup> Calcd for C<sub>21</sub>H<sub>20</sub>NO<sub>2</sub> 318.1494; Found 318.1478.

2-Phenoxy-*N*-(4-phenoxyphenyl)acetamide (ST48): Obtained following the general synthesis method A from 2-phenoxyacetyl chloride (theoretically 1 mmol), 1a (1 mmol), and DIPEA (1.5 mmol). Yield: 62%, white solid. Mp 137.3-137.5 °C. <sup>1</sup>H NMR (DMSO-*d*<sub>6</sub>, 500 MHz): δ 10.10 (s, 1H), 7.67 (d, *J*=8.9 Hz, 2H), 7.37 (t, *J*=8.0 Hz, 2H), 7.33 (t, *J*=8.0 Hz, 2H), 7.11 (t, *J*=7.4 Hz, 1H), 6.97-7.03 (m, 7H), 4.70 (s, 2H). <sup>13</sup>C NMR (DMSO-*d*<sub>6</sub>, 125 MHz): δ 166.9, 158.3, 157.7, 152.6, 134.7, 130.4, 130.0, 123.5, 122.0, 121.7, 119.8, 118.4, 115.2, 67.7. HRMS (ESI/TOF) *m/z*: [M+H]<sup>+</sup> Calcd for C<sub>20</sub>H<sub>18</sub>NO<sub>3</sub> 320.1287; Found 320.1295.

2-(Methyl(phenyl)amino)-*N*-(4-phenoxyphenyl)acetamide (ST49): A solution of *N*-methylaniline (1.1 mmol) and DIPEA (1.1 mmol) in ACN was stirred at room temperature for 15 min. After adding 1b (1 mmol), the reaction was stirred overnight at 50 °C. Upon completion of the reaction, the reaction mixture was diluted with DCM and subjected to sequential washing with 1% aqueous solution of NaHCO<sub>3</sub> and brine. After being dried over anhydrous Na<sub>2</sub>SO<sub>4</sub>, the combined organic phase was concentrated *in vacuo*. The crude product underwent purification via silica-based column chromatography using an elution system of *n*-hexane:ethyl acetate (80:20) to afford ST49. Yield: 24%, white solid. Mp 134.8-135.5 °C. <sup>1</sup>H NMR (CDCl<sub>3</sub>, 400 MHz): δ 8.42 (br s, 1H), 7.47-7.51 (d, *J*=9.2 Hz, 2H), 7.26-7.34 (t, *J*=7.6 Hz, 4H), 7.09 (t, *J*=7.2 Hz, 1H), 6.96-7.01 (m, 4H), 6.91 (t, *J*=7.6 Hz, 1H), 6.84 (d, *J*=9.2 Hz, 2H), 3.97 (s, 2H), 3.09 (s, 3H). <sup>13</sup>C NMR (CDCl<sub>3</sub>, 100 MHz): δ 168.6, 157.5, 153.7, 149.4, 132.7, 129.7, 129.5, 123.1, 121.6, 119.6, 119.4, 118.4, 113.7, 60.0, 40.1. HRMS (ESI/TOF) *m/z*: [M+H]<sup>+</sup> Calcd for C<sub>21</sub>H<sub>21</sub>N<sub>2</sub>O<sub>2</sub> 333.1603; Found 333.1610.

*N*-(4-Phenoxyphenyl)-5-phenylthiophene-2-carboxamide (ST50): Obtained following the general synthesis method B from 5-phenylthiophene-2-car-

boxylic acid (1 mmol), HOBt (1 mmol), EDC (1 mmol), DIPEA (1.5 mmol), and **1a** (1 mmol). Yield: 59%, white solid. Mp 197.4-197.8 °C. <sup>1</sup>H NMR (DMSO-*d*<sub>6</sub>, 500 MHz): δ 10.29 (s, 1H), 8.03 (d, *J*=3.9 Hz, 1H), 7.71 (d, *J*=8.6 Hz, 4H), 7.64 (d, *J*=3.9 Hz, 1H), 7.48 (t, *J*=7.4 Hz, 2H), 7.39 (t, *J*=7.9 Hz, 3H), 7.13 (t, *J*=7.4 Hz, 1H), 7.05 (d, *J*=8.6 Hz, 2H), 7.01 (d, *J*=7.9 Hz, 2H). <sup>13</sup>C NMR (DMSO-*d*<sub>6</sub>, 125 MHz): δ 160.0, 157.7, 152.9, 148.8, 139.3, 134.9, 133.5, 130.6, 130.5, 129.8, 129.2, 126.2, 124.9, 123.6, 122.6, 119.7, 118.6. HRMS (ESI/TOF) *m/z*: [M+H]<sup>+</sup> Calcd for C<sub>23</sub>H-<sub>18</sub>NO<sub>2</sub>S 372.1058; Found 372.1059.

*N*-(4-Phenoxyphenyl)benzothiophene-2-carboxamide (ST51): Obtained following the general synthesis method B from benzothiophene-2-carboxylic acid (1 mmol), HOBt (1 mmol), EDC (1 mmol), DIPEA (1.5 mmol), and **1a** (1 mmol). Yield: 54%, white solid. Mp 192.2-193.1 °C. <sup>1</sup>H NMR (DMSO-*d*<sub>6</sub>, 500 MHz): δ 10.56 (s, 1H), 8.36 (s, 1H), 8.06 (d, *J*=7.4 Hz, 1H), 8.02 (d, *J*=8.4 Hz, 1H), 7.80 (d, *J*=9.0 Hz, 2H), 7.48-7.51 (m, 2H), 7.40 (t, *J*=8.4 Hz, 2H), 7.13 (t, *J*=7.4 Hz, 1H), 7.07 (d, *J*=9.0 Hz, 2H), 7.02 (d, *J*=7.8 Hz, 2H). <sup>13</sup>C NMR (DMSO-*d*<sub>6</sub>, 125 MHz): δ 160.6, 157.6, 152.9, 140.9, 140.5, 139.6, 134.9, 130.5, 127.0, 126.2, 125.9, 125.5, 123.6, 123.3, 122.5, 119.7, 118.6. HRMS (ESI/TOF) *m/z*: [M+H]<sup>+</sup> Calcd for C<sub>21</sub>H<sub>16</sub>NO<sub>2</sub>S 346.0902; Found 346.0903.

*N*-(4-Phenoxyphenyl)-5-phenylfuran-2-carboxamide (ST52): Obtained following the general synthesis method A, from 5-phenylfuran-2-carbonyl chloride (theoretically 1 mmol), **1a** (1 mmol), and DIPEA (1.5 mmol). Yield: 42%, yellowish oil. <sup>1</sup>H NMR (DMSO-*d*<sub>6</sub>, 500 MHz): δ 10.21 (s, 1H), 7.98 (d, *J*=7.2 Hz, 2H), 7.79 (d, *J*=9.0 Hz, 2H), 7.51 (t, *J*=7.4 Hz, 2H), 7.36-7.44 (m, 4H), 7.18 (d, *J*=3.6 Hz, 1H), 7.13 (t, *J*=7.4 Hz, 1H), 7.06 (d, *J*=9.0 Hz, 2H), 7.02 (dd, *J*=8.7 and 1.0 Hz, 2H). <sup>13</sup>C NMR (DMSO-*d*<sub>6</sub>, 125 MHz): δ 157.7, 156.4, 155.7, 152.9, 147.1, 134.6, 130.5, 129.8, 129.4, 129.2, 125.0, 123.6, 122.9, 119.7, 118.6, 117.4, 108.3. HRMS (ESI/TOF) *m/z*: [M+H]<sup>+</sup> Calcd for C<sub>23</sub>H<sub>18</sub>NO<sub>3</sub> 356.1287; Found 356.1301.

*N*-(4-Phenoxyphenyl)benzofuran-2-carboxamide (ST53): Obtained following the general synthesis method A from benzofuran-2-carbonyl chloride (theoretically 1 mmol), **1a** (1 mmol), and DIPEA (1.5 mmol). Yield: 66%, white solid. Mp 159.0-159.4 °C. <sup>1</sup>H NMR (DMSO-*d*<sub>6</sub>, 500 MHz): δ 10.59 (s, 1H), 7.83-7.86 (m, 3H), 7.77 (d, *J*=0.8 Hz, 1H), 7.73 (dd, *J*=8.4 and 0.8 Hz, 1H), 7.51 (t, *J*=7.4 Hz, 1H), 7.35-7.43 (m, 3H), 7.13 (tt, *J*=7.4 and 1.1 Hz, 1H), 7.06 (d, *J*=9.0 Hz, 2H), 7.01 (d, *J*=7.7 Hz, 2H). <sup>13</sup>C NMR (DMSO-*d*<sub>6</sub>, 125 MHz): δ 157.6, 157.0, 154.9, 153.0, 149.3, 134.6, 130.5, 127.6, 124.3, 123.6 (2C), 123.4, 122.7, 119.7, 118.6, 112.4, 111.1. HRMS (ESI/TOF) *m/z*: [M+H]<sup>+</sup> Calcd for C<sub>21</sub>H<sub>16</sub>NO<sub>3</sub> 330.1130; Found 330.1126.

*N*-(4-(Benzyloxy)phenyl)-2-(phenylthio)acetamide (ST54): Obtained following the general synthesis method A, from 2-(phenylthio)acetyl chloride (theoretically 1 mmol), 4-(benzyloxy)aniline (1 mmol), and DIPEA (1.5 mmol). Yield: 28%, white solid. Mp 150.3-150.8 °C. <sup>1</sup>H NMR (DMSO-*d*<sub>6</sub>, 400 MHz): δ 10.07 (s, 1H), 7.30-7.47 (m, 11H), 7.20 (t, *J*=7.2 Hz, 1H), 6.95 (d, *J*=8.8 Hz, 2H), 5.06 (s, 2H), 3.82 (s, 2H). <sup>13</sup>C NMR (DMSO-*d*<sub>6</sub>, 100 MHz): δ 166.3, 154.4, 137.1, 135.9, 132.1, 129.0, 128.4, 128.0, 127.8, 127.7, 125.9, 120.7, 114.9, 69.3, 37.3. HRMS (ESI/TOF) *m/z*: [M+H]<sup>+</sup> Calcd for C<sub>21</sub>H<sub>20</sub>NO<sub>2</sub>S 350.1215; Found 350.1215.

*N*-(4-(Phenoxymethyl)phenyl)-2-(phenylthio)acetamide (ST55): Obtained following the general synthesis method A, from 2-(phenylthio)acetyl chloride (theoretically 1 mmol), 4-(phenoxymethyl)aniline (1 mmol), and DIPEA (1.5 mmol). Yield: 24%, white solid. Mp 139.5-139.8 °C. <sup>1</sup>H NMR (DMSO-*d*<sub>6</sub>, 400 MHz): δ 10.25 (s, 1H), 7.56 (d, *J*=8.2 Hz, 2H), 7.38 (t, *J*=8.0 Hz, 4H), 7.27-7.33 (m, 4H), 7.19 (t, *J*=7.2 Hz, 1H), 6.98 (d, *J*=8.2 Hz, 2H), 6.92 (t, *J*=7.2 Hz, 1H), 5.01 (s, 2H), 3.85 (s, 2H). <sup>13</sup>C NMR (DMSO-*d*<sub>6</sub>, 100 MHz): δ 166.7, 158.2, 138.4, 135.8, 132.0, 129.4, 128.9, 128.4, 128.0, 125.9, 120.5, 119.0, 114.7, 68.7, 37.4. HRMS (ESI/TOF) *m/z*: [M+H]<sup>+</sup> Calcd for C<sub>21</sub>H-<sub>20</sub>NO<sub>2</sub>S 350.1215; Found 350.1216.

*N*-(4-(Phenylamino)phenyl)-2-(phenylthio)acetamide (ST56): Obtained following the general synthesis method A, from 2-(phenylthio)acetyl chloride (theoretically 1 mmol), *N*-phenyl-1,4-phenylenediamine (1 mmol), and DIPEA (1.5 mmol). Yield: 42%, white solid. Mp 145.0-145.1 °C. <sup>1</sup>H NMR (DMSO-*d*<sub>6</sub>, 500 MHz): δ 10.01 (s, 1H), 8.03 (s, 1H), 7.41-7.45 (m, 4H), 7.33 (t, *J*=7.8 Hz, 2H), 7.19- 7.23 (m, 3H), 7.00-7.04 (m, 4H), 6.78 (t, *J*=7.3 Hz, 1H), 3.83 (s, 2H). <sup>13</sup>C NMR (DMSO-*d*<sub>6</sub>, 125 MHz): δ 166.6, 144.4, 139.6, 136.5, 132.1, 129.6, 129.5, 128.5, 126.4, 121.0, 119.6, 118.2, 116.4, 37.9. HRMS (ESI/TOF) *m/z*: [M+H]<sup>+</sup> Calcd for C<sub>21</sub>H<sub>19</sub>N<sub>2</sub>S 335.1218; Found 335.1228.

*N*-(4-(Benzylamino)phenyl)-2-(phenylthio)acetamide (ST57): A solution of benzaldehyde (1 mmol), 2b (1 mmol), and anhydrous Na<sub>2</sub>SO<sub>4</sub> (6 mmol) in DCM was stirred at room temperature under an argon atmosphere until imine formation was completed. Following the filtration of the reaction mixture, the imine intermediate (filtrate) was concentrated *in vacuo* and dissolved in methanol. Then, NaBH<sub>4</sub> was slowly added and stirred for 30 min at room temperature. After the reaction was completed, the mixture was diluted with a 5% aqueous solution of NaHCO<sub>3</sub> until pH≈8 and subjected to extracting with DCM (3x10 ml). After being dried over anhydrous Na<sub>2</sub>SO<sub>4</sub>, the combined organic phase was concentrated *in vacuo*. The crude underwent purification via silica-based column chromatography using an elution system of *n*-hexane:ethyl acetate (85:15) to afford ST57. Yield: 24%, white solid. Mp 124.8-125.1 °C. <sup>1</sup>H NMR (DMSO-*d*<sub>6</sub>, 500 MHz): δ 9.78 (s, 1H), 7.38-7.41 (m, 2H), 7.30-7.36 (m, 6H), 7.18-7.23 (m, 4H), 6.52 (d, *J*=8.9 Hz, 2H), 6.10 (t, *J*=6.0 Hz, 1H), 4.24 (d, *J*=6.0 Hz, 2H), 3.78 (s, 2H). <sup>13</sup>C NMR (DMSO-*d*<sub>6</sub>, 125 MHz): δ 166.2, 145.7, 140.8, 136.6, 129.4, 128.7, 128.5, 128.4, 127.6, 127.0, 126.3, 121.4, 112.6, 47.2, 37.8. HRMS (ESI/TOF) *m/z*: [M+H]<sup>+</sup> Calcd for C<sub>21</sub>H<sub>21</sub>N<sub>2</sub>OS 349.1375; Found 349.1364.

*N*-(4-((Phenylamino)methyl)phenyl)-2-(phenylthio)acetamide (ST58): A solution of aniline (1 mmol), 2c (1 mmol), and anhydrous Na<sub>2</sub>SO<sub>4</sub> (6 mmol)

in DCM was stirred at room temperature under an argon atmosphere until imine formation was completed. Following the filtration of the reaction mixture, the imine intermediate (filtrate) was concentrated *in vacuo* and dissolved in methanol. Then, NaBH<sub>4</sub> was slowly added and stirred for 30 min at room temperature. After the reaction was completed, the mixture was diluted with a 5% aqueous solution of NaHCO<sub>3</sub> until pH≈8 and subjected to extracting with DCM (3x10 ml). After being dried over anhydrous Na<sub>2</sub>SO<sub>4</sub>, the combined organic phase was concentrated *in vacuo*. The crude product underwent purification via silica-based column chromatography using an elution system of DCM:methanol (99:1) to afford ST58. Yield: 43%, white solid. Mp >300 °C. <sup>1</sup>H NMR (DMSO-*d*<sub>6</sub>, 500 MHz): δ 10.26 (s, 1H), 7.50 (d, *J*=8.5 Hz, 2H), 7.40 (d, *J*=7.4 Hz, 2H), 7.32 (t, *J*=7.8 Hz, 2H), 7.29 (d, *J*=8.5 Hz, 2H), 7.20 (t, *J*=7.4 Hz, 1H), 7.03 (t, *J*=7.8 Hz, 2H), 6.55 (d, *J*=7.8 Hz, 2H), 6.50 (t, *J*=7.4 Hz, 1H), 6.15 (t, *J*=5.8 Hz, 1H), 4.19 (d, *J*=5.8 Hz, 2H), 3.85 (s, 2H). <sup>13</sup>C NMR (DMSO-*d*<sub>6</sub>, 125 MHz): δ 167.1, 149.1, 137.9, 136.4, 135.8, 129.5, 129.3, 128.5, 128.0, 126.5, 119.7, 116.2, 112.7, 46.5, 37.9. HRMS (ESI/TOF) *m/z*: [M+H]<sup>+</sup> Calcd for C<sub>21</sub>H<sub>21</sub>N<sub>2</sub>OS 349.1375; Found 349.1369.

*N*-(4-Benzylphenyl)-2-(phenylthio)acetamide (ST59): Obtained following the general synthesis method A, from 2-(phenylthio)acetyl chloride (theoretically 1 mmol), 4-benzylaniline (1 mmol), and DIPEA (1.5 mmol). Yield: 40%, white solid. Mp 136.0-136.3 °C. <sup>1</sup>H NMR (DMSO-*d*<sub>6</sub>, 400 MHz): δ 10.09 (s, 1H), 7.47 (d, *J*=8.4 Hz, 2H), 7.40 (d, *J*=7.6 Hz, 2H), 7.31 (t, *J*=8.4 Hz, 2H), 7.26 (d, *J*=7.6 Hz, 2H), 7.14-7.21 (m, 6H), 3.88 (s, 2H), 3.83 (s, 2H). <sup>13</sup>C NMR (DMSO-*d*<sub>6</sub>, 100 MHz): δ 166.5, 141.3, 136.8, 136.3, 135.8, 128.9 (2C), 128.5, 128.3, 128.0, 125.9, 125.8, 119.3, 40.4, 37.4. HRMS (ESI/TOF) *m/z*: [M+H]<sup>+</sup> Calcd for C<sub>21</sub>H<sub>20</sub>NOS 334.1266; Found 334.1258.

*N*-(4-Benzoylphenyl)-2-(phenylthio)acetamide (ST60): Obtained following the general synthesis method A, from 2-(phenylthio)acetyl chloride (theoretically 1 mmol), 4-aminobenzophenone (1 mmol),

and DIPEA (1.5 mmol). Yield: 32%, white solid. Mp 130.7-131.1 °C. <sup>1</sup>H NMR (DMSO-*d*<sub>6</sub>, 400 MHz): δ 10.60 (s, 1H), 7.64-7.77 (m, 7H), 7.55 (t, *J*=7.6 Hz, 2H), 7.41 (d, *J*=8.0 Hz, 2H), 7.33 (t, *J*=7.6 Hz, 2H), 7.21 (t, *J*=7.6 Hz, 1H), 3.92 (s, 2H). <sup>13</sup>C NMR (DM-SO-*d*<sub>6</sub>, 100 MHz): δ 194.5, 167.5, 142.9, 137.5, 135.6, 132.3, 131.6, 131.2, 129.4, 129.1, 128.5, 128.2, 126.1, 118.4, 37.6. HRMS (ESI/TOF) *m/z*: [M+H]<sup>+</sup> Calcd for C<sub>21</sub>H<sub>18</sub>NO<sub>2</sub>S 348.1058; Found 348.1064.

#### ***In vitro* SIRT2 inhibition assay**

The inhibitory activities of the title compounds were examined using SIRT2 Direct Fluorescent Screening Assay Kits (Item No. 700280) following the manufacturer's protocol (Cayman Chemical, Ann Arbor, MI, USA) and a previously reported method (Gozelle et al., 2023). The percentage of inhibition in each well was calculated by comparing the fluorescence readings of compound-treated wells to those of control wells. The experiment was repeated three times.

#### **Molecular docking**

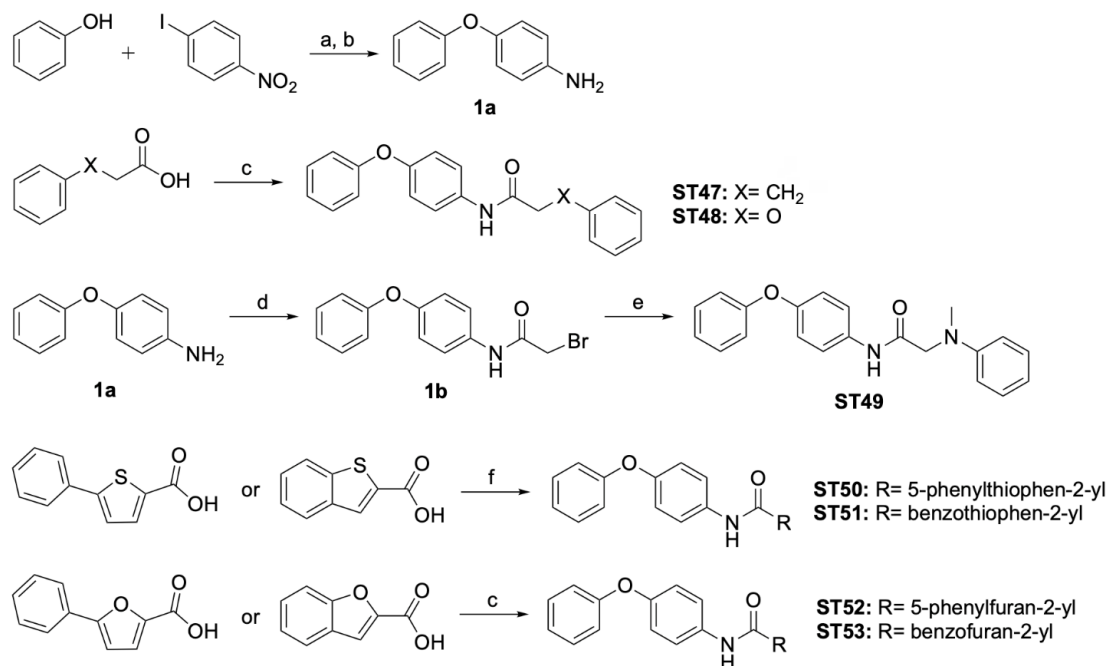
The molecular docking simulations were performed using Glide within the Schrödinger Small-Molecule Drug Discovery Suite (Small-Molecule Drug Discovery Suite 2023-1, Schrödinger, LLC, New York, NY, 2023). The x-ray crystal structure of human SIRT2 (PDB: 5DY4) was retrieved from the RCSB Protein Data Bank and prepared by our previous protocol (Gozelle et al., 2022). The selected compounds were docked into the SIRT2 active site using

the XP docking mode using a radius scaling factor of 0.80 vdW and a partial charge cutoff of 0.20 (Friesner et al., 2006).

## **RESULTS AND DISCUSSION**

### **Synthesis**

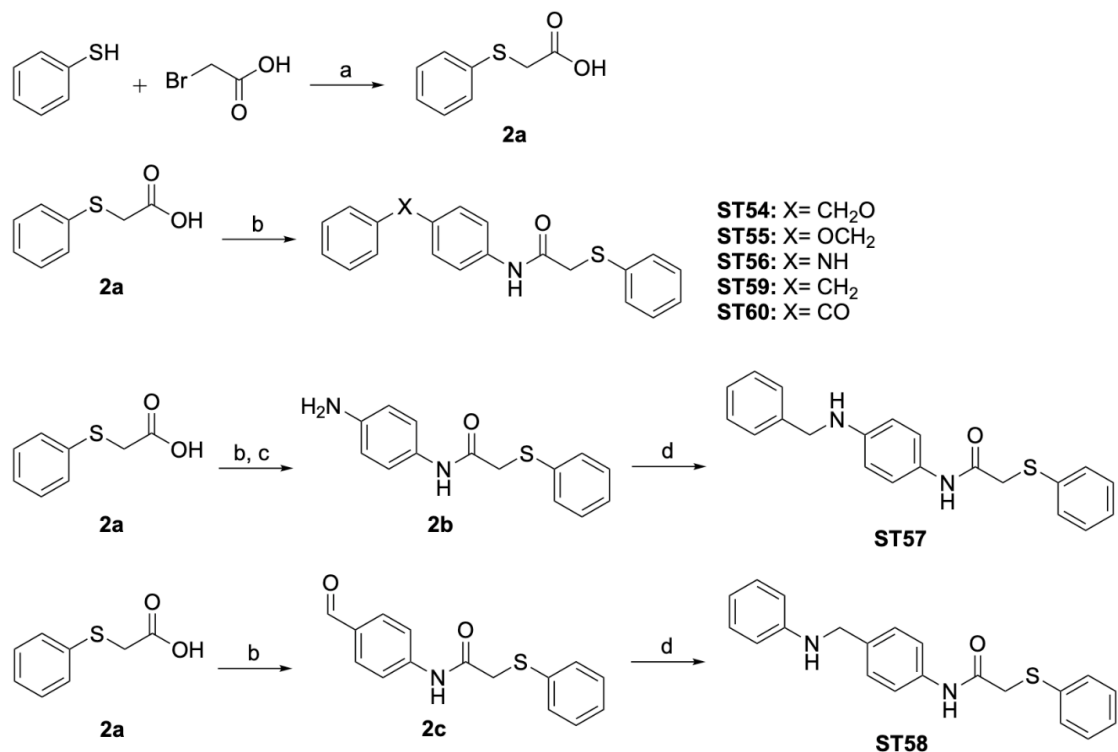
The synthesis of *N*-(4-phenoxyphenyl)aryl-carboxamide derivatives (**ST47-ST53**) was carried out following the synthetic sequence depicted in Scheme 1. The Ullman coupling reaction of commercially available 1-iodo-4-nitrobenzene and phenol, catalyzed by CuI and *N,N*-dimethylglycine, afforded 1-nitro-4-phenoxybenzene, which was used without further purification in the next step. 4-Phenoxyaniline (**1a**) was obtained by reduction of the 1-nitro-4-phenoxybenzene in the presence of SnCl<sub>2</sub>·2H<sub>2</sub>O. The title compounds **ST47**, **ST48**, **ST52**, and **ST53** were synthesized by the reaction of **1a** with an appropriate acyl chloride, which was produced in the presence of oxalyl chloride from commercially available carboxylic acid derivatives with total yields ranging from 42% to 66%. **ST49** was obtained through the substitution reaction of *N*-methylaniline and the 2-bromo-*N*-(4-phenoxyphenyl)acetamide intermediate (**1b**), which was the product of the reaction between **1a** and 2-bromoacetyl bromide in a yield of 24%. Moreover, amide coupling reactions of 5-phenylthiophene-2-carboxylic acid or benzothiophene-2-carboxylic acid with **1a** in the presence of EDC, HOBt, and DIPEA afforded the desired compounds **ST50** or **ST51** with 54% and 59% yields, respectively.



**Scheme 1.** Synthetic route to compounds **ST47–ST53**. Reagents and conditions: (a) CuI, Cs<sub>2</sub>CO<sub>3</sub>, *N,N*-dimethylglycine, 1,4-dioxane, DMF, 100 °C, overnight; (b) SnCl<sub>2</sub>·2H<sub>2</sub>O, ethanol, reflux, 4 h; (c) *i.* appropriate carboxylic acid (3-phenylpropanoic acid for **ST47**, 2-phenoxyacetic acid for **ST48**, 5-phenylfuran-2-carboxylic acid for **ST52**, benzofuran-2-carboxylic acid for **ST53**), oxalyl chloride, cat. DMF, DCM, rt, 2 h, *ii.* **1a**, DIPEA, DCM, rt, 2–4 h; (d) 2-bromoacetyl bromide, TEA, rt, 3 h; (e) *N*-methylaniline, DIPEA, ACN, 100 °C, overnight; (f) appropriate carboxylic acid (5-phenylthiophene-2-carboxylic acid for **ST50** and benzothiophene-2-carboxylic acid for **ST51**), **1a**, EDC, HOBT, DIPEA, DCM, rt, overnight.

The synthesis of *N*-(aryl)-2-(phenylthio)acetamides was carried out under the synthetic sequence depicted in Scheme 2. Initially, 2-(phenylthio)acetic acid (**2a**), which is the starting material for *N*-(aryl)-2-(phenylthio)acetamide derivatives, was synthesized through the reaction of thiophenol and 2-bromoacetic acid in a basic medium. Subsequently, by reacting commercially available 4-substituted aniline derivatives with 2-(phenylthio)acetyl chloride, which was obtained from **2a** and oxalyl chloride, the desired compounds **ST54**, **ST55**, **ST56**, **ST59**, and **ST60** were produced with total yields ranged from 24% to 42%. The first step in the synthesis route to **ST57** was the reaction of 2-(phenylthio)acetyl chloride with 4-nitroaniline, yielding *N*-(4-nitrophenyl)-2-(phenylthio)acetamide. Next, by reducing nitro precursor in the

presence of SnCl<sub>2</sub>·2H<sub>2</sub>O, *N*-(4-aminophenyl)-2-(phenylthio)acetamide (**2b**) was obtained in a yield of 55%. An indirect reductive amination procedure involving the condensation of **2b** with benzaldehyde and the subsequent reduction with NaBH<sub>4</sub> gave the desired product **ST57** with a 61% yield. In the case of compound **ST58**, 4-aminobenzaldehyde was reacted with 2-(phenylthio)acetyl chloride yielding *N*-(4-formylphenyl)-2-(phenylthio)acetamide (**2c**), which was used in the next step without further purification, followed by an indirect reductive amination reaction of **2c** and aniline producing the title compound **ST58** in a yield of 43%. Finally, the structures of the final compounds were confirmed by <sup>1</sup>H-NMR, <sup>13</sup>C-NMR, and HRMS spectra.



**Scheme 2.** Synthetic route to compounds **ST54-ST60**. Reagents and conditions: (a) NaOH, K<sub>2</sub>CO<sub>3</sub>, ethanol, water, rt, 2 h; (b) *i.* **2a**, oxalyl chloride, cat. DMF, DCM, rt, 2 h, *ii.* Appropriate amine (4-(benzyloxy)aniline for **ST54**, 4-(phenoxyethyl)aniline for **ST55**, *N*-phenyl-*p*-phenylenediamine for **ST56**, 4-benzylaniline for **ST59**, 4-aminobenzophenone for **ST60**, 4-nitroaniline for **2b**, 4-aminobenzaldehyde for **2c**), DIPEA, DCM, rt, 2-4 h; (c) SnCl<sub>2</sub>·2H<sub>2</sub>O, ethanol, reflux, 6 h; (d) *i.* benzaldehyde for **ST57**, aniline for **ST58**, Na<sub>2</sub>SO<sub>4</sub>, DCM, rt, overnight, *ii.* NaBH<sub>4</sub>, methanol, rt, 30 min.

### Biological results

The inhibitory activities of the target compounds (**ST47-ST60**) against SIRT2 were tested in a fluorescence-based assay (Damonte et al., 2017; Yoon & Kim, 2016) at a screening dose of 100 μM. The results are listed in Table 1. According to the results, a significant increase in the inhibition rates of the tested compounds was observed compared to that of STH2.

A brief overview of SAR related to the modifications performed revealed that among the compounds **ST47-ST49** generated by bioisosteric replacement of sulfur atom close to the tail group, **ST49** with *N*-methylamino group exhibited the best inhibition rate with a value of 50.07% at 100 μM. In comparison, STH2 had an inhibition value of 84.28% and 36.89% against SIRT2 at 300 μM and 100 μM screening con-

centrations, respectively. The title compounds **ST50-ST53** bearing thiophene, benzothiophene, furan, and benzofuran rings were obtained due to fused ring cyclization and chain cyclization strategies implemented through the tail group. The fused ring compounds (**ST51** and **ST53**) demonstrated a slight superiority in SIRT2 inhibitory effect compared to **ST50** and **ST52** with 5-phenylthiophene and 5-phenylfuran moieties, respectively. Besides, **ST50** and **ST51**, with sulfur-containing rings, were more likely to show potent inhibition against SIRT2 than their counterparts with oxygen-containing rings (**ST52** and **ST53**). Regarding the linker modification, the title compounds **ST54-ST60** were obtained to contain various linkers instead of oxygen atom in the STH2 structure. Surprisingly, replacement of oxygen linker with -CH<sub>2</sub>O- and

-OCH<sub>2</sub>- groups in ST54 and ST55 led to significant loss of inhibitory effect on SIRT2 activity, while **ST56**, ST57, and ST58 with amine-containing linker (-NH-, -CH<sub>2</sub>NH-, -NHCH<sub>2</sub>-) displayed an enhanced SIRT2 inhibition ranging from 27.81% to 42.31% at 100 μM screening concentration. Moreover, SIRT2 inhibitions of 41.52% and 54.03% were obtained at 100 μM methylene linker-bearing ST59 and carbonyl linker-bearing ST60, respectively. Compared to the data gained in our previous study (Gozelle et al., 2023), the analogs with thiophene as the central ring exhibited a more potent inhibitory effect against SIRT2. In addition, the introduction of longer linker groups (n=2) resulted in a decrease in activity. All compounds tested displayed moderate inhibitory activity against

SIRT2 compared to Suramin, the non-selective sirtuin inhibitor with an IC<sub>50</sub> value of 1.15 μM for SIRT2 (Trapp et al., 2007).

The compounds exhibiting 47-54% SIRT2 inhibition (ST49, ST51, ST60) were evaluated for their *in vitro* SIRT1 and SIRT3 inhibitory activities to predict the isoform selectivity. The results showed that all three compounds did not show significant inhibitory potency against SIRT1 compared to the selective SIRT1 inhibitor EX-527, which had an IC<sub>50</sub> value of 0.28 nM (Broussy, Laaroussi, & Vidal, 2020; Solomon et al., 2006). Furthermore, none of the compounds tested showed significant inhibitory potency against SIRT3, confirming the accuracy of our design approach to selectively inhibit SIRT2.

**Table 1.** *In vitro* inhibitory profiles of compounds tested at 100  $\mu$ M against SIRT2

ID	X	R	%inhibition $\pm$ SD			Modification
			SIRT2	SIRT1	SIRT3	
ST47			29.73 $\pm$ 4.88	n.t.	n.t.	
ST48			40.15 $\pm$ 1.75	n.t.	n.t.	
ST49			50.07 $\pm$ 2.07	8.54 $\pm$ 3.50	19.98 $\pm$ 4.09	
ST50	-O-		41.66 $\pm$ 5.13	n.t.	n.t.	tail group
ST51			47.19 $\pm$ 5.92	7.29 $\pm$ 4.05	18.10 $\pm$ 3.23	
ST52			30.45 $\pm$ 0.64	n.t.	n.t.	
ST53			39.93 $\pm$ 4.21	n.t.	n.t.	
ST55	-CH <sub>2</sub> O-		n.i.	n.t.	n.t.	
ST56	-OCH <sub>2</sub> -		n.i.	n.t.	n.t.	
ST54	-NH-		33.57 $\pm$ 4.60	n.t.	n.t.	
ST57	-CH <sub>2</sub> NH-		27.81 $\pm$ 0.32	n.t.	n.t.	linker
ST58	-NHCH <sub>2</sub> -		42.31 $\pm$ 7.24	n.t.	n.t.	
ST59	-CH <sub>2</sub> -		41.52 $\pm$ 7.13	n.t.	n.t.	
ST60	-CO-		54.03 $\pm$ 1.52	n.i.	19.17 $\pm$ 0.14	
STH2	-O-		84.28 $\pm$ 5.19* 36.89 $\pm$ 0.45	n.i.	n.i.	-
EX-527	-	-	76.39 $\pm$ 2.49	99.28 $\pm$ 1.07	44.61 $\pm$ 3.81	-
Suramin	-	-	98.37 $\pm$ 0.25	94.52 $\pm$ 0.92	96.82 $\pm$ 3.26	-

SD: standard deviation ( $n = 3$ ); \* Percent inhibition @300  $\mu$ M; n.i.: no inhibition; n.t.: not tested.

### Molecular modelling

To predict the orientations of synthesized compounds bound to SIRT2, molecular docking studies were carried out compared to the binding pose of STH2. The information gathered from the x-ray crystal structure of SIRT2 (PDB: 5DY4) highlighted the importance of the critical interactions, including  $\pi$ - $\pi$  stacking with F119, F131, and F234 at the entrance of

the substrate binding channel,  $\pi$ - $\pi$  stacking with Y139 and F190 at the selectivity pocket, and water-mediated H-bonding with P94 (Schiedel et al., 2016).

Although molecular docking is a valuable tool for understanding ligand binding predictions, it regularly fails to differentiate active from inactive compounds within each chemical family (Chen, 2015). In our case, the docking results, especially for ST60, could not pro-

vide supportive findings to establish a relationship between the binding conformation varying according to chemical structure and the inhibitory effect.

The SIRT2:docked STH2 complex showed that all critical interactions mentioned above were obtained. The replacement of 2-(4-isopropyl-4*H*-1,2,4-triazol-3-yl)thio moiety, the so-called tail group, by 2-methyl(phenyl)amino (ST49) led to the loss of interaction with F131 in the substrate channel, maintaining the water-mediated H-bond with P94. ST60, exhibiting the best inhibitory profile in the series, unexpectedly occupied the active site by interacting only with F190 in the selectivity pocket and F119 in the substrate binding channel. It was suggested that the reduced rotation of phenyl rings due to introducing the carbonyl

group into the linker induced a conformational modification, yielding less interaction in the entrance of the substrate channel (Figure 2). The most notable conformational change is observed for the compounds with fused rings on the tail group (ST51 and ST53). Benzothiophene and benzofuran ring systems, which were used in fused ring cyclization, accessed the deeper inside the selectivity pocket due to the formation of more favorable  $\pi$ - $\pi$  contacts than those of compounds with 5-phenylthiophene and 5-phenylfuran moieties (ST50 and ST52). They adopted less bent conformation that prevented interaction with P94 *via* structural water (Figure S4). The binding energies for STH2, ST49, and ST60 in the SIRT2 active site were calculated as -10.77, -11.43, and -10.82 kcal/mol, respectively.

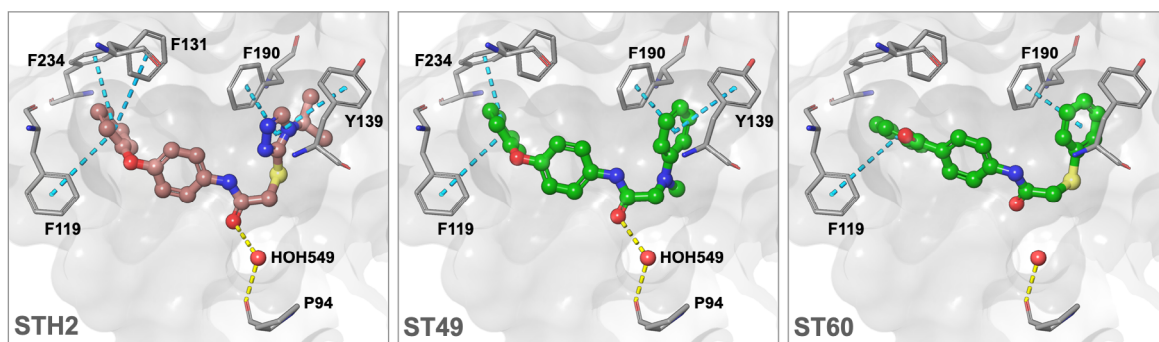


**Figure 2.** The proposed binding modes of docked compounds in the SIRT2 active site (PDB: 5DY4). H-bonds and  $\pi$ - $\pi$  contacts are represented by yellow and cyan dashed-lines, respectively.

## CONCLUSION

In this work, we aimed to find analogs that exhibit more potent inhibition of SIRT2 by modifying the linker and tail groups on our initial virtual screening-derived hit. This eventually resulted in a significant increase in SIRT2 inhibitory activity. Our best SIRT2 inhibitors, **ST49** and **ST60**, exhibited 50.07% and 54.03% inhibition at 100  $\mu$ M, respectively, while **STH2** inhibited SIRT2 by 84.28% and 36.89% at 300 and 100  $\mu$ M screening concentrations, respectively. Moreover, ST49 and ST60 showed no significant inhibitory effect against SIRT1 and SIRT3 isoforms. Based on these findings, it may be suggested that the one-atom linker led to tighter binding to SIRT2 and more potent inhi-

bition than the two-atom linker. Besides, the impact of the tail group involving  $\pi$  systems on inhibition ability was undeniable as maintaining the crucial  $\pi$ - $\pi$  contacts with the aromatic residues of the selectivity pocket. This study, however, offers essential insights into structure-guided modifications for further hit expansion in the design of SIRT2 inhibitors.

## ACKNOWLEDGMENT

Financial support by the Scientific and Technological Research Council of Turkey (TUBITAK) under Grant 118S673 is gratefully acknowledged.

## CONFLICT OF INTEREST

The authors declare that there is no conflict of interest.

#### AUTHOR CONTRIBUTION STATEMENT

M.G.: Methodology, Investigation, Writing-Original Draft. Y.O: Methodology. G.E.: Conceptualization, Supervision, Methodology, Writing-Original Draft, Writing-Review & Editing. All authors reviewed the results and approved the final version of the manuscript.

#### REFERENCES

- Avalos, J. L., Celic, I., Muhammad, S., Cosgrove, M. S., Boeke, J. D., & Wolberger, C. (2002). Structure of a Sir2 Enzyme Bound to an Acetylated p53 Peptide. *Molecular Cell*, 10(3), 523-535. doi:10.1016/S1097-2765(02)00628-7
- Biswas, S., & Rao, C. M. (2018). Epigenetic tools (The Writers, The Readers and The Erasers) and their implications in cancer therapy. *European Journal of Pharmacology*, 837, 8-24. doi:10.1016/j.ejphar.2018.08.021
- Broussy, S., Laaroussi, H., & Vidal, M. (2020). Biochemical mechanism and biological effects of the inhibition of silent information regulator 1 (SIRT1) by EX-527 (SEN0014196 or selisistat). *Journal of Enzyme Inhibition and Medicinal Chemistry*, 35(1), 1124-1136. https://doi.org/10.1080/14756366.2020.1758691
- Cai, H., Wang, Y., Zhang, J., Wei, Z., Yan, T., Feng, C., . . . Wu, Y. (2023). Discovery of Novel SIRT1/2 Inhibitors with Effective Cytotoxicity against Human Leukemia Cells. *Journal of Chemical Information and Modeling*, 63(15), 4780-4790. doi:10.1021/acs.jcim.3c00556
- Chen, B., Zang, W., Wang, J., Huang, Y., He, Y., Yan, L., . . . Zheng, W. (2015). The chemical biology of sirtuins. *Chemical Society Reviews*, 44(15), 5246-5264. doi:10.1039/C4CS00373J
- Chen, G., Huang, P., & Hu, C. (2020). The role of SIRT2 in cancer: A novel therapeutic target. *International Journal of Cancer*, 147(12), 3297-3304. doi:10.1002/ijc.33118
- Chen, Y. C. (2015). Beware of docking! *Trends in Pharmacological Sciences*, 36(2), 78-95. doi:10.1016/j.tips.2014.12.001
- Damonte, P., Sociali, G., Parenti, M. D., Soncini, D., Bauer, I., Boero, S., . . . Bruzzone, S. (2017). SIRT6 inhibitors with salicylate-like structure show immunosuppressive and chemosensitizing effects. *Bioorganic & Medicinal Chemistry*, 25(20), 5849-5858. doi:10.1016/j.bmc.2017.09.023
- Eren, G., Bruno, A., Guntekin-Ergun, S., Cetin-Atalay, R., Ozgencil, F., Ozkan, Y., . . . Costantino, G. (2019). Pharmacophore modeling and virtual screening studies to identify novel selective SIRT2 inhibitors. *Journal of Molecular Graphics & Modelling*, 89, 60-73. doi:10.1016/j.jmgm.2019.02.014
- Friesner, R. A., Murphy, R. B., Repasky, M. P., Frye, L. L., Greenwood, J. R., Halgren, T. A., . . . Mainz, D. T. (2006). Extra Precision Glide: Docking and Scoring Incorporating a Model of Hydrophobic Enclosure for Protein-Ligand Complexes. *Journal of Medicinal Chemistry*, 49, 6177-6196. doi:10.1021/jm051256o
- Frye, R. A. (2000). Phylogenetic Classification of Prokaryotic and Eukaryotic Sir2-like Proteins. *Biochemical and Biophysical Research Communications*, 273(2), 793-798. doi:10.1006/bbrc.2000.3000
- Ganesan, A., Arimondo, P. B., Rots, M. G., Jeronimo, C., & Berdasco, M. (2019). The timeline of epigenetic drug discovery: from reality to dreams. *Clinical Epigenetics*, 11(1), 174. doi:10.1186/s13148-019-0776-0

- Gozelle, M., Kaya, S. G., Aksel, A. B., Ozkan, E., Bakar-Ates, F., Ozkan, Y., & Eren, G. (2022). Hit evaluation results in 5-benzyl-1,3,4-thiadiazole-2-carboxamide based SIRT2-selective inhibitor with improved affinity and selectivity. *Bioorganic Chemistry*, *123*, 105746. doi:10.1016/j.bioorg.2022.105746
- Gozelle, M., Bakar-Ates, F., Massarotti, A., Ozkan, E., Gunindi, H. B., Ozkan, Y., & Eren, G. (2023). In silico approach reveals N-(5-phenoxythiophen-2-yl)-2-(arylthio)acetamides as promising selective SIRT2 inhibitors: the case of structural optimization of virtual screening-derived hits. *Journal of Biomolecular Structure and Dynamics*, 1-12. doi:10.1080/07391102.2023.2293252
- Han, M., Han, Y., Song, C., & Hahn, H.-G. (2012). The Design and Synthesis of 1,4-Substituted Piperazine Derivatives as Triple Reuptake Inhibitors. *Bulletin of the Korean Chemical Society*, *33*(8), 2597-2602. doi:10.5012/bkcs.2012.33.8.2597
- Hong, J. Y., Fernandez, I., Anmangandla, A., Lu, X., Bai, J. J., & Lin, H. (2021). Pharmacological Advantage of SIRT2-Selective versus pan-SIRT1-3 Inhibitors. *ACS Chemical Biology*, *16*(7), 1266-1275. doi:10.1021/acscmbio.1c00331
- Jing, E. X., Gesta, S., & Kahn, C. R. (2007). SIRT2 regulates adipocyte differentiation through FoxO1 acetylation/deacetylation. *Cell Metabolism*, *6*(2), 105-114. doi:10.1016/j.cmet.2007.07.003
- Kaya, S. G., & Eren, G. (2023). Selective inhibition of SIRT2: A disputable therapeutic approach in cancer therapy. *Bioorg Chem*, *143*, 107038. doi:10.1016/j.bioorg.2023.107038
- Lanning, M. E., Yu, W., Yap, J. L., Chauhan, J., Chen, L., Whiting, E., . . . Fletcher, S. (2016). Structure-based design of N-substituted 1-hydroxy-4-sulfamoyl-2-naphthoates as selective inhibitors of the Mcl-1 oncoprotein. *European Journal of Medicinal Chemistry*, *113*, 273-292. doi:10.1016/j.ejmech.2016.02.006
- Lu, Y., Chan, Y.-T., Tan, H.-Y., Li, S., Wang, N., & Feng, Y. (2020). Epigenetic regulation in human cancer: the potential role of epi-drug in cancer therapy. *Molecular Cancer*, *19*(1), 79. doi:10.1186/s12943-020-01197-3
- Ma, D., Cai, Q. (2003). N,N-Dimethyl Glycine-Promoted Ullmann Coupling Reaction of Phenols and Aryl Halides. *Organic Letters*, *5*(21), 3799-3802. doi:10.1021/ol0350947
- Mellini, P., Itoh, Y., Tsumoto, H., Li, Y., Suzuki, M., Tokuda, N., . . . Suzuki, T. (2017). Potent mechanism-based sirtuin-2-selective inhibition by an in situ-generated occupant of the substrate-binding site, "selectivity pocket" and NAD<sup>+</sup>-binding site. *Chemical Science*, *8*(9), 6400-6408. doi:10.1039/C7SC02738A
- Min, J. S., Kim, J. C., Kim, J. A., Kang, I., & Ahn, J. K. (2018). SIRT2 reduces actin polymerization and cell migration through deacetylation and degradation of HSP90. *Biochimica Et Biophysica Acta-Molecular Cell Research*, *1865*(9), 1230-1238. doi:10.1016/j.bbamcr.2018.06.005
- North, B. J., Marshall, B. L., Borra, M. T., Denu, J. M., & Verdin, E. (2003). The Human Sir2 Ortholog, SIRT2, Is an NAD<sup>+</sup>-Dependent Tubulin Deacetylase. *Molecular Cell*, *11*(2), 437-444. doi:10.1016/S1097-2765(03)00038-8
- North, B. J., Rosenberg, M. A., Jeganathan, K. B., Hafner, A. V., Michan, S., Dai, J., . . . Sinclair, D. A. (2014). SIRT2 induces the checkpoint kinase BubR1 to increase lifespan. *The EMBO journal*, *33*(13), 1438-1453. doi:10.15252/embj.201386907
- Penteado, A. B., Hassanie, H., Gomes, R. A., Emery, F. d. S., & Trossini, G. H. G. (2023). Human sirtuin 2 inhibitors, their mechanisms and binding modes. *Future Medicinal Chemistry*, *15*(3), 291-311. doi:10.4155/fmc-2022-0253

- Quinti, L., Casale, M., Moniot, S., Pais, Teresa F., Van Kanegan, Michael J., Kaltenbach, Linda S., . . . Kazantsev, Aleksey G. (2016). SIRT2- and NRF2-Targeting Thiazole-Containing Compound with Therapeutic Activity in Huntington's Disease Models. *Cell Chemical Biology*, 23(7), 849-861. doi:10.1016/j.chembiol.2016.05.015
- Rumpf, T., Schiedel, M., Karaman, B., Roessler, C., North, B. J., Lehotzky, A., . . . Jung, M. (2015). Selective Sirt2 inhibition by ligand-induced rearrangement of the active site. 6, 6263. doi:10.1038/ncomms7263
- Schiedel, M., Rumpf, T., Karaman, B., Lehotzky, A., Oláh, J., Gerhardt, S., . . . Jung, M. (2016). Aminothiazoles as Potent and Selective Sirt2 Inhibitors: A Structure-Activity Relationship Study. *Journal of Medicinal Chemistry*, 59(4), 1599-1612. doi:10.1021/acs.jmedchem.5b01517
- Silva, R. d. F. e., Bassi, G., Câmara, N. O. S., & Moretti, N. S. (2023). Sirtuins: Key pieces in the host response to pathogens' puzzle. *Molecular Immunology*, 160, 150-160. doi:10.1016/j.molimm.2023.06.010
- Solomon, J. M., Pasupuleti, R., Liu, X., McDonagh, T., Curtis, R., DiStefano, P. S., & Huber, L. (2006). Inhibition of SIRT1 Catalytic Activity Increases p53 Acetylation but Does Not Alter Cell Survival following DNA Damage. *Molecular and Cellular Biology*, 26(1), 28-38. https://doi.org/10.1128/mcb.26.1.28-38.2006
- Spiegelman, N. A., Hong, J. Y., Hu, J., Jing, H., Wang, M., Price, I. R., . . . Lin, H. N. (2019). A Small-Molecule SIRT2 Inhibitor That Promotes K-Ras4a Lysine Fatty-Acylation. *ChemMedChem*, 14(7), 744-748. doi:10.1002/cmdc.201800715
- Sukuroglu, M. K., Gozelle, M., Ozkan, Y., & Eren, G. (2021). The potential of 4-aryl-6-morpholino-3(2H)-pyridazinone-2-arylpiperazinylacetamide as a new scaffold for SIRT2 inhibition: in silico approach guided by pharmacophore mapping and molecular docking. *Medicinal Chemistry Research*, 30(10), 1915-1924. doi:10.1007/s00044-021-02782-x
- Tantawy, A. H., Meng, X.-G., Marzouk, A. A., Fouad, A., Abdelazeem, A. H., Youssif, B. G. M., . . . Wang, M.-Q. (2021). Structure-based design, synthesis, and biological evaluation of novel piperine-resveratrol hybrids as antiproliferative agents targeting SIRT-2. *RSC Advances*, 11(41), 25738-25751. doi:10.1039/D1RA04061H
- Trapp, J., Jochum, A., Meier, R., Saunders, L., Marshall, B., Kunick, C., . . . Jung, M. (2006). Adenosine Mimetics as Inhibitors of NAD<sup>+</sup>-Dependent Histone Deacetylases, from Kinase to Sirtuin Inhibition. *Journal of Medicinal Chemistry*, 49(25), 7307-7316. doi:10.1021/jm060118b
- Trapp, J., Meier, R., Hongwiset, D., Kassack, M. U., Sippl, W., & Jung, M. (2007). Structure-Activity studies on suramin analogues as inhibitors of NAD<sup>+</sup>-Dependent histone deacetylases (Sirtuins). *ChemMedChem*, 2(10), 1419-1431. https://doi.org/10.1002/cmdc.200700003
- Wang, Y., Yang, J., Hong, T., Chen, X., & Cui, L. (2019). SIRT2: Controversy and multiple roles in disease and physiology. *Ageing Research Reviews*, 55, 100961. doi:10.1016/j.arr.2019.100961
- Xie, Y., Yang, Y., Li, S., Xu, Y., Lu, W., Chen, Z., . . . Bian, X. (2017). Phenylsulfonylfuroxan NO-donor phenols: Synthesis and multifunctional activities evaluation. *Bioorganic and Medicinal Chemistry*, 25(16), 4407-4413. doi:10.1016/j.bmc.2017.06.023
- Xu, Y., Li, F., Lv, L., Li, T., Zhou, X., Deng, C.-X., . . . Xiong, Y. (2014). Oxidative Stress Activates SIRT2 to Deacetylate and Stimulate Phosphoglycerate Mutase. *Cancer Research*, 74(13), 3630. doi:10.1158/0008-5472.CAN-13-3615
- Yagci, S., Gozelle, M., Kaya, S. G., Ozkan, Y., Aksel, A. B., Bakar-Ates, F., . . . Eren, G. (2021). Hit-to-lead optimization on aryloxybenzamide derivative virtual screening hit against SIRT. *Bioorganic & Medicinal Chemistry*, 30, 115961. doi:10.1016/j.bmc.2020.115961

- Yang, L.-L., Wang, H.-L., Zhong, L., Yuan, C., Liu, S.-Y., Yu, Z.-J., . . . Li, G.-B. (2018). X-ray crystal structure guided discovery of new selective, substrate-mimicking sirtuin 2 inhibitors that exhibit activities against non-small cell lung cancer cells. *European Journal of Medicinal Chemistry*, 155, 806-823. doi:10.1016/j.ejmech.2018.06.041
- Yang, L. L., Xu, W., Yan, J., Su, H. L., Yuan, C., Li, C., . . . Li, G.-B. (2019). Crystallographic and SAR analyses reveal the high requirements needed to selectively and potently inhibit SIRT2 deacetylase and decanoylase. *Medchemcomm*, 10(1), 164-168. doi:10.1039/c8md00462e
- Yoon, S. P., & Kim, J. (2016). Poly(ADP-ribose) polymerase 1 contributes to oxidative stress through downregulation of sirtuin 3 during cisplatin nephrotoxicity. *Anatomy & cell biology*, 49(3), 165-176. doi:10.5115/acb.2016.49.3.165
- Zhang, D., Zhang, J., Wang, Y., Wang, G., Tang, P., Liu, Y., . . . Ouyang, L. (2023). Targeting epigenetic modifications in Parkinson's disease therapy. *Medicinal Research Reviews*, 43(5), 1748-1777. doi:10.1002/med.21962
- Zhao, D., Zou, S.-W., Liu, Y., Zhou, X., Mo, Y., Wang, P., . . . Guan, K.-L. (2013). Lysine-5 Acetylation Negatively Regulates Lactate Dehydrogenase A and Is Decreased in Pancreatic Cancer. *Cancer Cell*, 23(4), 464-476. doi: 10.1016/j.ccr.2013.02.005